Stress-Induced Crystallization of Poly(Trimethylene Terephthalate) Fibers by Molecular Dynamic Simulations

Min-Kang Hsieh and Shiang-Tai Lin,
Department of Chemical Engineering, National Taiwan University, Taipei, Taiwan

Introduction

The phenomena of stress-induced (or flow-induced, strain-induced, force-induced) crystallization is characterized by the preferential of orientation of polymer segments along the direction of applied force. Many researches report that the drawing and spinning process would increase the crystallinity of polymeric materials, resulting in oriented segments that would explosively improve the crystallization by oriented nuclei.

There are many works showing the evidences of the structural changes during drawing and spinning processes. From the behavior of stress-draw ratio curve of the melt-quenched amorphous PTT film during uniaxial drawing, a significant strain hardening could be observed simultaneously with crystallinity (measured by density) abruptly rising after draw ratio of 2.5.[1,2] Besides, the development of oriented structure has been quantified by orientation factor calculated from IR dichrocic ratio of characteristic bands[3] and intensity of WXRD[4] of the melt-quenched amorphous PTT. Moreover, the birefringence of PTT increases with spinning speeds.[5] On the other hand, many theoretical works on stress-induced crystallization using molecular simulations, most of which focus on linear polyethylene (PE). It is found that the torsional ordering[6] and is followed by increase in orientation factor[7] in the simulation with the pre-oriented models. The shish-kebab crystallization was observed by extensional flow process,[8] and the secondary nucleation around a knot in the polymer system has been studied.[9]

The change in the torsional conformation of a propylene glycol segment (O-CH_2-CH_2-CH_2-O) during the drawing or spinning process is of great interest. The torsion angle distribution of the segment has been reported as *tans-gauche-gauche-trans* (t-g-g-t) in the crystalline state.[10,11] However, what the distribution in amorphous state is and how they transfer form amorphous to crystalline state remain unclear. The conformation of amorphous state may either be dominated by *g-t-t-g,* state[3] or in random[12] states; some even estimated the content of the gauche state of ϕ_2 to be 33.4%.[2] Furthermore, the mechanism of the conformation transition from amorphous to crystalline phase has been studied using IR spectroscopy[2,3,12-14], X-ray scatting[15], and ^{13}C solid-state NMR.[16] Form those resuts, in crystalline phase, the ϕ_2 exists largely in the *gauche* state, and ϕ_1 conformation exists largely in the *trans* state. In amorphous phase, ϕ_2 conformation exists mostly in the *trans* state, but ϕ_1 conformation is unclear. Moreover, during the annealing process, ϕ_2 conformation changes form *trans* state to *gauche* state but ϕ_1 conformation is unclear. During drawing process, ϕ_2 conformation changes form *trans* state to *gauche* state, if polymer chains undergo sufficient thermal relaxation; however, ϕ_1 conformation is unclear.

In this work we focus on the development of ordering of structures in the stress-induced crystallization process. (The thermal effect of the development ordering structure has been studied in our previous works.) The temperature dependence of the amount of ordered clusters, the behavior of ordered structures and torsion angle transition during drawing and annealing processes are analyzed. The results

presented here help us better understand the mechanism of the nucleation at the early stage of crystallization.

Computational methods

Atomistic molecular dynamic simulations are used to study the dynamic behavior of the nucleation process. The molecular models of PTT are prepared using commercial package Cerius2.[17] Each model contains 4 chains of PTT molecules, each having a degree of polymerization of 27. Thus each unit cell contains 108 repeating units of PTT, or equivalently 2708 atoms. In all the simulations, the generic force field Dreiding[18] is used to describe the interactions among atoms in a system. The potential energy includes the bond stretching energy (U_b), angle bending energy (U_θ), torsional angle rotation energy (U_ϕ), electrostatic interaction (U_{coul}), and van der Waals interactions (U_{vdw}). Atomic (Mulliken) charges are determined from density functional theory (DFT) calculations for the monomer of PTT using the B3LYP functional and 6-31G** basis set in Gaussian 98[19]. Moreover, the torsion terms of the propylene glycol segment (O-CH_2-CH_2-CH_2-O) being modified to better reproduce quantum mechanics (QM) results, according the energy barrier results of rotating torsion angles.[20] This force field could reproduce reasonably the thermal properties (Tm and Tg), mechanical property (Young's modulus), and crystal structural properties.[20]

The computer code LAMMPS [21] is used for all subsequent molecular dynamic simulations. A series of expansion and compression steps were applied to the initial structures in order to obtain equilibrium samples at 600K (which is above the melting temperature T_m). The 100 ps equilibrated sample is then cooled to 50 K at a rate of 1 K/ps. At each 50 K interval during the quenching process, the samples are then drawn with different drawing speeds ($1x10^8 s^{-1}$(only at 400K), $1x10^9 s^{-1}$, $1x10^{10} s^{-1}$, and $1x10^{11} s^{-1}$), and isothermally relaxed at several draw ratios (DR=1, 2, 3, and 4) up to 12 ns with pressure at 0 bar and $NTL_x\sigma_{yy}\sigma_{zz}$ ensemble with zero normal stress in y and z directions.[22] Nose-Hoover thermostat is used for temperature control. The integration time step used is 0.5 to 1 fs.

Results and discussions

Bulk Properties

The changes in bulk properties are observed (Fig. 1) during stress-induced crystallization in our simulation. The increase of the amount of precursors in the draw process is much more remarkable than that in isothermal crystallization. Furthermore, the subsequent process of relaxation (NVT simulation after the drawing process) would lead to further increase in the fraction of oriented precursors. The rapid density decrease in each simulation indicates that the defects (voids) in the bulk phase are created during the drawing processes. At high draw speeds ($1x10^{10}$ s^{-1}, and $1x10^{11}$ s^{-1}) and the temperatures below T_g the formation of defects is prominent; on the other hand, at the slower draw speeds ($1x10^8$ s^{-1}, and $1x10^9$ s^{-1}) and temperatures above T_g the system relaxation is fast enough to reduce the amount of defects.

The changes in van der Waals interaction and the torsional energy reflect the transition of the structure under various drawing conditions. The van der Waals interaction increases with DR in all cases. These interaction energies also have a significant effect in the system density. For example, the

relaxation of van der Waals interaction leads to a constant density at lower draw speed ($1x10^9$ s^{-1}). A rapid increase in van der Waals interaction leads to a rapid drop in density at higher draw speed ($1x10^{11}$ s^{-1}). Besides, the van der Waals interaction increases with temperature at constant DR. The enhancement of van der Waals interactions slows down at temperatures higher than T_g at lower draw speed. These results indicate that the mechanism of the chain packing is different in the various draw speeds and temperatures. This could be understood as a competition between thermal effect, which is prominent at slower draw speed and higher temperatures, and stress effect, which is prominent at faster draw speed and lower temperatures. On the other hand, the torsional energy decreases with DR at lower draw speeds ($1x10^9$ s^{-1}, and $1x10^{10}$ s^{-1}), but fluctuates at the highest draw speed ($1x10^{11}$ s^{-1}). It is almost a linear function of temperature at constant DR. These results support that the stress effect influents the backbone chain rotation much more than thermal effect.

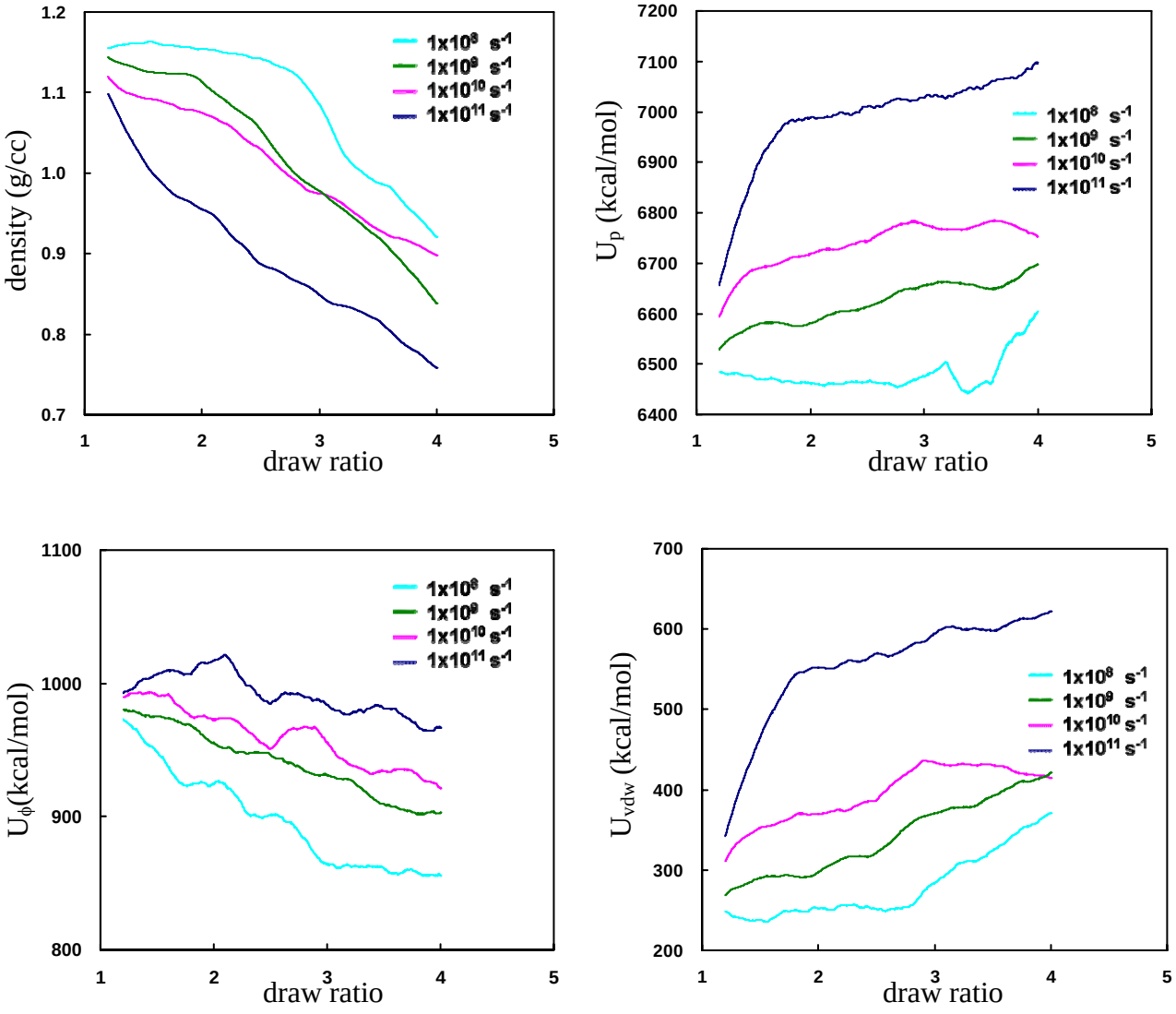

Figure1 The energy and density of the overall system.

The Fraction of Ordering Structure

The fraction of ordering structure, *X*, has been defined in previous work.[20] As shown in Fig. 2, at small DR (DR=2), the fraction of precursors increases in all temperatures with slower draw speeds ($1x10^{9}s^{-1}$ and $1x10^{10}s^{-1}$), but decreases at temperatures 350K and 400K with higher draw speed ($1x10^{11}s^{-1}$). At larger DR (DR>3), the saturation of induced precursor is observed for all temperatures with the slowest draw speed ($1x10^{9}s^{-1}$). On the other hand, the development of precursors continues at the higher draw speed ($1x10^{10}s^{-1}$ and $1x10^{10}s^{-1}$). Besides, the orientation factor increases with DR, and the curves are similar in all situations, indicating that the orientation factor may be a function of draw ratio only. This implies that the stress-induced precursor is similar at the same DR with each draw speed.

The subsequent thermal relaxation (following the drawing process) could stabilize and facilitate in the growth of oriented precursors. The results of the fraction of precursors shows a temperature depence similar to that of the isothermal crystallization, but the position of highest amount of precursors shifts to a lower temperature (300K with drawing vs 400 K without drawing[20]). The local motion of polymer segments would be induced by uni-axis stress. (Note the maximum capacity of precursor formation should be found between the temperature allowing for short rage motion and that for entire chain motion.)

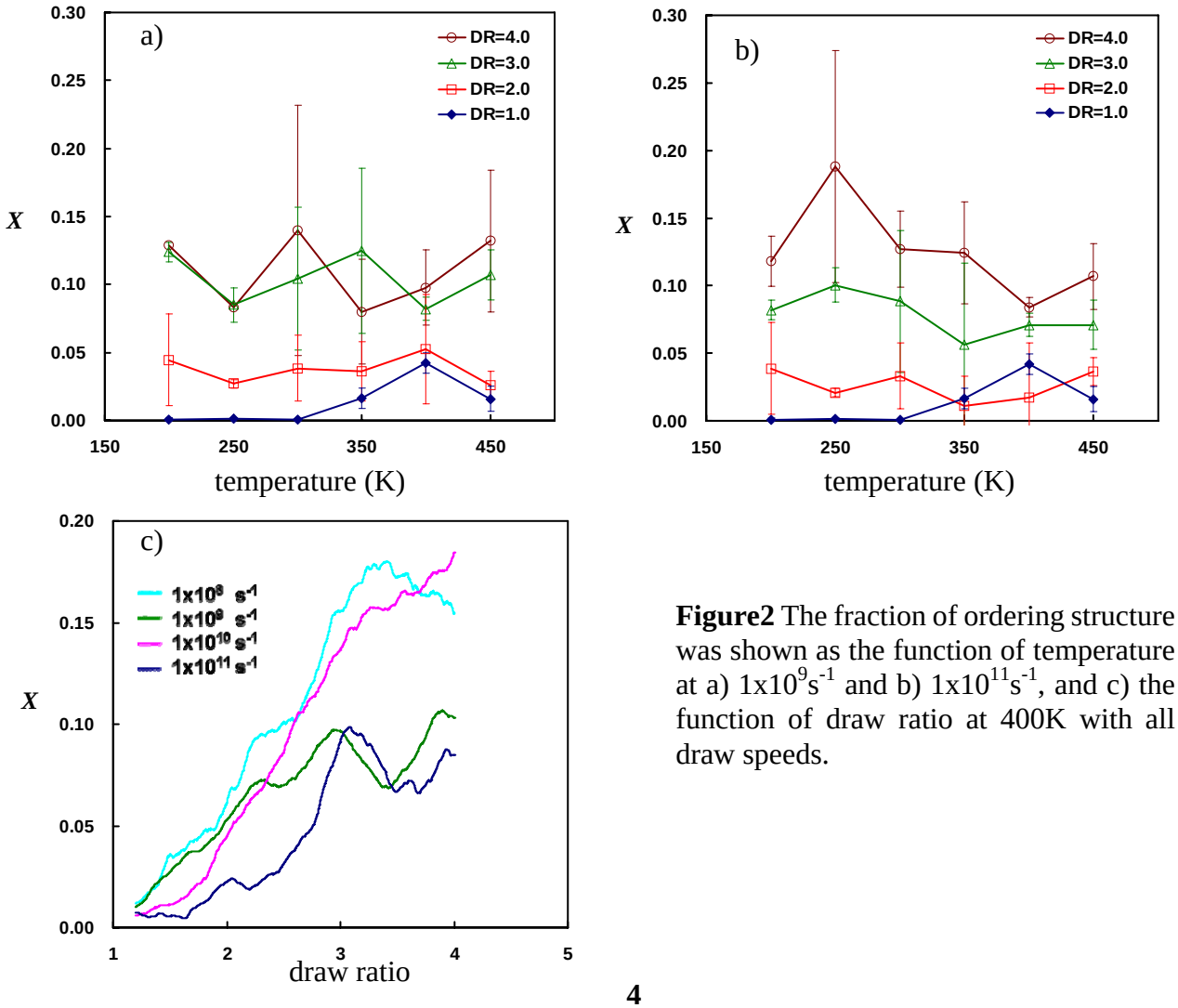

Figure2 The fraction of ordering structure was shown as the function of temperature at a) $1x10^{9}s^{-1}$ and b) $1x10^{11}s^{-1}$, and c) the function of draw ratio at 400K with all draw speeds.

The trosional angle distribution

To understand the distribution of torsional angles in the PTT backbone (O-CH_2-CH_2-CH_2-O), we analyze the percentage of the trans and gauche states during the stress-induced crystallization. Different behaviors observed at different draw speeds. The percentage of ϕ_1 and ϕ_2 in trans state fluctuates at small DR, and increases at larger DR with slower draw speed. At higher draw speeds, this percentage decreases at small DR and increases at larger DR. The percentage value rebounds to the original value with draw speed $1x10^{11}s^{-1}$. On the other hand, the percentage of gauche state decreases with DR at all draw speeds. During thermal relaxation, the percentage of the trans rebounds in all draw speeds, but that of gauche rebounds only in faster draw speed. These results suggest that torsional angles change to transition state in the beginning drawing process, and then become trans state at higher DR or under thermal relaxation.

Detailed analysis also is performed on the two feature torsions (ϕ_1 and ϕ_2) in the PTT backbone (Fig. 3). It is found that the trans-to-gauche ratio in ϕ_1 increases rapidly (from 3 to 6) at lower drawing speed and higher temperatures; however, the increase is less significant at high drawing speed and low temperatures. In contrast, the gauche-to-trans ratio for ϕ_2 seems to be insensitive to processing conditions (varies from 1.6 to 0.8 regardless of drawing speeds). After thermal relaxation, the value of trans-to-gauche ratio in ϕ_1 improves significantly in the slower draw speeds, but remains almost constant in the fastest draw speed. On the other hand, the gauche-to-trans ratio for ϕ_2 decreases at small DR with slower draw speeds ($1x10^{9}s^{-1}$ and $1x10^{10}s^{-1}$), but increases at larger DR with faster draw speed.

Before drawing, the fraction of trans state is ~34%, and that of gauche is ~25% in the bulk phase; the most populated conformations in ϕ_1 is trans, and that in ϕ_2 is gauche; i.e., the most populated conformations in the backbone torsions are t-g-g-t (ϕ_1- ϕ_2- ϕ_2- ϕ_1). During draw process, the t-t-t-t conformation increases. Our results are in agreement with the result of Chuch's experimental observation.[14] The thermal relaxation would change the conformations in some of our simulations, but the changes are not obvious.

The states of backbone torsional angles in precursors evolve with DR differently in different processing conditions. The fraction of ϕ_1 in trans increases with DR, but the fraction of ϕ_2 in gauche decreases with DR in most precursors. The stress and thermal effects are different in these two torsional angles. Slower draw speed and lower temperature would improve the change of ϕ_1 to the trans state; on the other hand, the faster draw speed and medium temperatures would improve the change of ϕ_2 to the gauche state. Furthermore, the fraction of ϕ_1 in trans is very high (~70%) in each precursor, but the fraction of ϕ_2 in gauche only 20~30%. That indicates that the stress-induced transition in ϕ_2 is faster than that in ϕ_1. In addition, the faction of ϕ_2 in gauche fluctuates in some cases, indicating the torsional angle ϕ_2 would favorably move to the gauche after forcing to the trans state by the external stress.

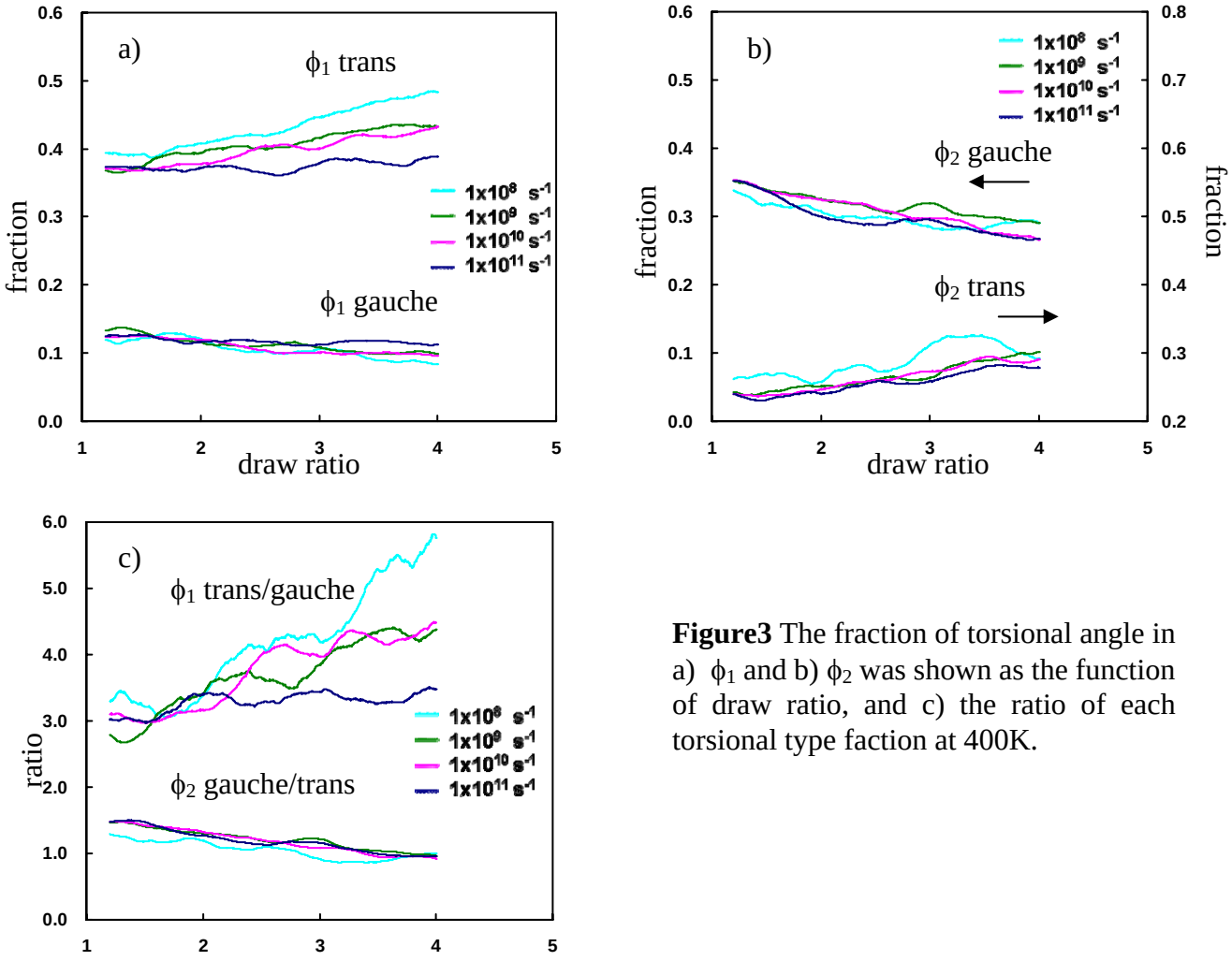

Figure3 The fraction of torsional angle in a) ϕ_1 and b) ϕ_2 was shown as the function of draw ratio, and c) the ratio of each torsional type faction at 400K.

Conclusion

The formation of oriented precursor in the stress-induced crystallization is observed in our simulation. The torsional and van der Waals forces are the dominant interactions, similar to the case observed in isothermal crystallization. The amount of stress-induced precursor increases in all regions of temperature. The maximum size of oriented precursor is larger than that created only by thermal stimulation. During stress-induced crystallization, the torsional distribution of the polymer backbone for segments rapidly rearrange to the t-t-t-t conformation in bulk phase. Within oriented precursors, the response of the torsional angle induced by stress is faster than that only induced by thermal stimulation, especially trans in ϕ_1(the transition rate of trans state in ϕ_1 is faster than that of gauche state in ϕ_2).

Acknowledgment

We would like to thank the financial support from Grant NSC 96-2221-E-002-106 by the National Science Council of Taiwan, and computation resources from the National Center for

High-Performance Computing of Taiwan.

References

1. Lee, H. S., S. C. Park and Y. H. Kim, "Structural changes of poly(trimethylene terephthalate) film upon uniaxial and biaxial drawing," *Macromolecules*, **33**, 7994 (2000).
2. Jeong, Y. G., W. J. Bae and W. H. Jo, "Effect of uniaxial drawing on surface chain structure and surface tension of poly(trimethylene terephthalate) film," *Polymer*, **46**, 8297 (2005).
3. Kim, K. J., J. H. Bae and Y. H. Kim, "Infrared spectroscopic analysis of poly(trimethylene terephthalate)," *Polymer*, **42**, 1023 (2001).
4. Wu, J., J. M. Schultz, J. M. Samon, et al., "In situ study of structure development in poly(trimethylene terephthalate) fibers during stretching by simultaneous synchrotron small- and wide-angle X-ray scattering," *Polymer*, **42**, 7141 (2001).
5.
6. Koyama, A., T. Yamamoto, K. Fukao, et al., "Molecular dynamics simulation of polymer crystallization from an oriented amorphous state," *Physical Review E*, **65**, (2002).
7. Lavine, M. S., N. Waheed and G. C. Rutledge, "Molecular dynamics simulation of orientation and crystallization of polyethylene during uniaxial extension," *Polymer*, **44**, 1771 (2003).
8. Dukovski, I. and M. Muthukumar, "Langevin dynamics simulations of early stage shish-kebab crystallization of polymers in extensional flow," *Journal of Chemical Physics*, **118**, 6648 (2003).
9. Saitta, A. M. and M. L. Klein, "Influence of a knot on the stretching-induced crystallization of a polymer," *Journal of Chemical Physics*, **116**, 5333 (2002).
10. Poulindandurand, S., S. Perez, J. F. Revol, et al., "Crystal-Structure of Poly(Trimethylene Terephthalate) by X-Ray and Electron-Diffraction," *Polymer*, **20**, 419 (1979).
11. Desborough, I. J., I. H. Hall and J. Z. Neisser, "Structure of Poly(Trimethylene Terephthalate)," *Polymer*, **20**, 545 (1979).
12. Ohtaki, M., T. Kameda, T. Asakura, et al., "Structural characterization of drawn and annealed poly(trimethylene terephthalate) fibers," *Polymer Journal*, **37**, 214 (2005).
13. Park, S. C., Y. R. Liang, H. S. Lee, et al., "Three-dimensional orientation change during thermally induced structural change of oriented poly(trimethylene terephthalate) films using polarized FTIR-ATR spectroscopy," *Polymer*, **45**, 8981 (2004).
14. Chuah, H. H., "Orientation and structure development in poly(trimethylene terephthalate) tensile drawing," *Macromolecules*, **34**, 6985 (2001).
15. Wu, J., J. M. Schultz, J. M. Samon, et al., "In situ study of structure development during continuous hot-drawing of poly(trimethylene terephthalate) fibers by simultaneous synchrotron small- and wide-angle X-ray scattering," *Polymer*, **42**, 7161 (2001).
16. Kameda, T., M. Miyazawa and S. Murase, "Conformation of drawn poly(trimethylene terephthalate) studied by solid-state C-13 NMR," *Magnetic Resonance in Chemistry*, **43**, 21 (2005).
17. Cerius2 (2003), Accelrys Inc., San Diego.
18. Mayo, S. L., Olafson, B. D. and Goddard, W. A. (1990), "*Dreiding - a Generic Force-Field for Molecular Simulations*," Journal of Physical Chemistry, pp. 8897-8909.
19. Gaussian 98 (2001), Revision A.11, Gaussian, Inc., Pittsburgh, PA.
20. Hsieh, M-K, and ST Lin, “Molecular Dynamic Simulations of Polymer Crystallization at the Early Stage”, AIChE annual meeting, 2007.

21. Plimpton, S. (1995), "*Fast Parallel Algorithms for Short-Range Molecular-Dynamics*," Journal of Computational Physics, pp. 1-19.
22. Capaldi, F. M., M. C. Boyce and G. C. Rutledge, "Molecular response of a glassy polymer to active deformation," Polymer, 45, 1391 (2004).